

Input Normalized Stochastic Gradient Descent Training for Deep Neural Networks

Anonymous authors

Paper under double-blind review

Abstract

In this paper, we propose a novel optimization algorithm for training machine learning models called Input Normalized Stochastic Gradient Descent (INSGD), inspired by the Normalized Least Mean Squares (NLMS) algorithm used in adaptive filtering. When training complex models on large datasets, the choice of optimizer parameters, particularly the learning rate, is crucial to avoid divergence. Our algorithm updates the network weights using stochastic gradient descent with ℓ_1 and ℓ_2 -based normalizations applied to the learning rate, similar to NLMS. However, unlike existing normalization methods, we exclude the error term from the normalization process and instead normalize the update term using the input vector to the neuron. Our experiments demonstrate that our optimization algorithm achieves higher accuracy levels compared to different initialization settings. We evaluate the efficiency of our training algorithm on benchmark datasets using ResNet-20, WResNet-18, ResNet-50, and a toy neural network. Our INSGD algorithm improves the accuracy of ResNet-20 on CIFAR-10 from 92.55% to 92.80%, the accuracy of MobileNetV3 on CIFAR-10 from 90.83% to 91.13%, WResNet-18 on CIFAR-100 from 78.75% to 78.85%, and ResNet-50 on ImageNet-1K from 75.56% to 75.89%.

1 Introduction

Deep Neural Networks (DNNs) have gained immense popularity and have been extensively applied across various research fields due to their convenience and ease of use in many machine learning tasks LeCun et al. (1995); He et al. (2016); Krizhevsky et al. (2017); Simonyan & Zisserman (2014); Long et al. (2015). Researchers from different domains can readily utilize DNN models for their work, as these models can adapt their parameters to find the best possible solutions for a wide range of problems, particularly in supervised learning scenarios. The parameters of a DNN model are updated using various optimization algorithms, and researchers have proposed different algorithms that offer fresh perspectives and address different conditions Ruder (2016). It is important to note that different optimization algorithms can yield different results in a given problem depending on the task at hand.

Stochastic Gradient Descent (SGD) is a widely adopted optimization algorithm for supervised learning in DNN models. It is a simple, efficient, and parallelizable algorithm that can produce very accurate results on large-scale datasets when appropriate initial conditions are set Bottou (2010). Another popular algorithm, called Adam, can outperform SGD in some cases; however, it is crucial to choose an initial learning rate carefully, as a relatively high value can lead to divergence Kingma & Ba (2014). While optimization algorithms play a significant role in training DNN models, ensuring convergence of weights and finding the optimal solution for a given problem is not always guaranteed. The evaluation of an optimization algorithm should also consider its limitations. This paper addresses two limitations in the convergence of deep neural network (DNN) models: the impact of different hyperparameter choices and the strength of the input signal. To overcome these limitations, we propose a novel optimization algorithm called Input Normalized Stochastic Gradient Descent (INSGD), which draws inspiration from the Normalized Least Mean Squares (NLMS) algorithm used in adaptive filtering Mathews & Xie (1993); Chan & Zhou (2010). Our study focuses on demonstrating how INSGD is inspired by NLMS and how it can effectively address problems caused by various factors.

The organization of the paper is as follows. In the following two subsections, we review the SGD and NLMS. In Section II, we introduce the Input Normalized Stochastic Gradient Descent (INSGD) algorithm. In Section III we present simulation examples and conclude the article in Section IV.

1.1 Stochastic Gradient Descent

Stochastic Gradient Descent (SGD) is an iterative optimization method commonly used in machine learning to update the weights of a network model. It calculates the gradient of the weights based on the objective function defined to measure the error in the training of the model and it estimates the new set of weights using the gradients with a predefined step size. The SGD can converge to the optimal or sub-optimal set of weights with the correct choice of step size and the initial settings when the cost function is convex Li & Orabona (2019) The gradual convergence provided by gradient descent helps us to optimize the weights used in any type of machine learning model.

Assume a pair of (\mathbf{x}, \mathbf{y}) composed of an arbitrary input \mathbf{x} and an output \mathbf{y} . Given a set of weights $\mathbf{w} \in \mathbb{W}$ where \mathbb{W} stands for the space of possible weights, a machine learning model predicts the output using a non-linear function $f(\mathbf{x}, \mathbf{w})$ and the optimal weights, \mathbf{w}^* , to minimize the objective (loss) function $L(\mathbf{y}, f(\mathbf{x}, \mathbf{w}))$

$$\mathbf{w}^* = \arg \min_{\mathbf{w} \in \mathbb{W}} L(\mathbf{y}, f(\mathbf{x}, \mathbf{w})). \quad (1)$$

Due to the highly complex and non-linear nature of machine learning models, it is impossible to find a closed-form solution for the optimization problem given in Eq. (1) ada (2008). The gradient descent algorithm is introduced to avoid extensive computation and give an iterative method to estimate the optimal weights. The formula for SGD is given as:

$$\mathbf{w}(k+1) = \mathbf{w}(k) + \lambda \nabla_{\mathbf{w}(k)} L(\mathbf{y}, f(\mathbf{x}, \mathbf{w})), \quad (2)$$

where $\mathbf{w}(j)$ represents the weights at j^{th} step, $\nabla_{\mathbf{w}(k)} L$ is the gradient of the objective function with respect to the weights being updated and λ is the step size or the learning rate.

Although SGD is a simple algorithm that can be applied to various tasks, it faces challenges related to tuning and scalability, which hinder its ability to converge quickly in deep learning algorithms. If the initial weights are not properly defined, and without preconditioned gradients that consider curvature information, the algorithm can become trapped in local minima Le et al. (2011); Hinton & Salakhutdinov (2006). To estimate the minimum of the objective function more effectively, a deeper understanding of the error surface is required. In addition to using gradients, the exploitation of second-order derivatives can lead to faster convergence however this requires calculating the Hessian matrix of the objective function. Calculating the second derivative with respect to each weight is computationally expensive and can lead to memory issues in deep networks. The Hessian matrix and its approximations are also utilized in the Normalized Least Mean Squares (NLMS)-type methods, which will be discussed in the following subsection.

1.2 Normalized Least Mean Squares (NLMS)

As pointed out above, the NLMS is widely used to estimate the weights of an adaptive filter, which is basically a linear neuron. In minimum mean square error filtering, assume \mathbf{u} , the input to a system, is a $1 \times M$ random vector with zero mean and a positive-definite covariance matrix $\mathbf{R}_{\mathbf{u}}$ and d , the desired output of the system, is a scalar random variable with zero mean and a finite variance σ_d^2 . The linear estimation problem is defined as the solution of

$$\min_{\mathbf{w}} \mathbb{E} |d - \mathbf{u}\mathbf{w}|^2, \quad (3)$$

where \mathbf{w} is a vector containing the filter coefficients to be optimized. The linear estimation problem declares the cost function as the mean-square error and it is defined as

$$J(w) = \mathbb{E} |d - \mathbf{u}\mathbf{w}|^2 = \mathbb{E}(d - \mathbf{u}\mathbf{w})(d - \mathbf{u}\mathbf{w})^T, \quad (4)$$

where $(.)^T$ denotes a transpose. If we expand Eq. (4), it is straightforward to obtain the cost function $J(w)$ in terms of the covariance and cross-covariance matrices:

$$J(w) = \sigma_d^2 - \mathbf{R}_{\mathbf{d}\mathbf{u}}^T \mathbf{w} - \mathbf{w}^T \mathbf{R}_{\mathbf{d}\mathbf{u}} + \mathbf{w}^T \mathbf{R}_{\mathbf{u}} \mathbf{w}, \quad (5)$$

where $\mathbf{R}_{\mathbf{d}\mathbf{u}} = \mathbb{E}[\mathbf{d}\mathbf{u}]$ is the cross-covariance matrix of d and \mathbf{u} . The closed-form solution to such a problem in (3) can be found using the linear estimation theory as $\mathbf{R}_{\mathbf{u}}\mathbf{w}^o = \mathbf{R}_{\mathbf{d}\mathbf{u}}$; however, it may not be possible to obtain a closed-form solution for problems with criteria other than the mean-square-error criterion.

The Least Mean Squares (LMS) algorithm, developed by Widrow *et al.* in the 1960s Widrow et al. (1960), computes the stochastic gradient and updates the weight vector iteratively to find a solution for the problem in (3). The weight vector can be updated using the following iterative process.

$$\mathbf{w}(j) = \mathbf{w}(j-1) + \lambda \mathbf{u}^T(j)\mathbf{e}(j), \quad (6)$$

where $\mathbf{u}(j)$ is j -th observation of the random vector \mathbf{u} and $\mathbf{e}(j) = \mathbf{d}(j) - \mathbf{u}^T\mathbf{w}(j-1)$ is the error vector at time j . The updating term is obtained as the negative of the stochastic gradient of the mean squared error function defined in Eq. (4) with respect to the weights.

The Normalized LMS (NLMS) algorithm has been shown to achieve a better convergence rate compared to LMS by incorporating a different step-size parameter for each component \mathbf{u}_i of the vector \mathbf{u} Sayed (2008). The LMS algorithm can encounter scalability issues when the input signal is large or when the step-size parameter is too large. Since the LMS algorithm uses a gradient-based approach to update the filter coefficients, and if the step-size parameter is too large, the filter coefficients can diverge. To address this, normalization is introduced to the update term:

$$\mathbf{w}(j) = \mathbf{w}(j-1) + \lambda \frac{\mathbf{e}(j)}{\|\mathbf{u}(j)\|_2^2} \mathbf{u}(j), \quad (7)$$

and the NLMS converges to the Wiener filter solution of the optimization problem in (3) as long as $0 < \lambda < 2$ Theodoridis et al. (2010); Yamada et al. (2002).

Another interpretation of the NLMS algorithm is based on the fact that the error $\mathbf{e}(j) = \mathbf{d}(j) - \mathbf{u}^T\mathbf{w}$ should be minimized by selecting an appropriate weight vector \mathbf{w} . The equation $\mathbf{d}(j) = \mathbf{u}^T\mathbf{w}$ is a hyperplane in the M dimensional weight space $\mathbf{w} \in \mathbb{R}^M$. When the vector $\mathbf{w}(j-1)$ is projected onto the hyperplane $\mathbf{e}(j) = \mathbf{d}(j) - \mathbf{u}^T\mathbf{w}$, we obtain the update equation:

$$\mathbf{w}(j) = \mathbf{w}(j-1) + \frac{\mathbf{e}(j)}{\|\mathbf{u}(j)\|_2^2} \mathbf{u}(j), \quad (8)$$

as shown in Fig. 1 and the error is minimized by selecting the next weight vector on the hyperplane $\mathbf{d}(j) = \mathbf{u}^T\mathbf{w}$. The orthogonal projection operation described in Eq. (8) minimizes the Euclidean distance between the vector $\mathbf{w}(j-1)$ and the hyperplane $\mathbf{d}(j) = \mathbf{u}^T\mathbf{w}$ Combettes (1993); Trussell & Civanlar (1984); Cetin et al. (1997; 2013) The weights converge to the intersection of the hyperplanes as shown in Fig. 1,

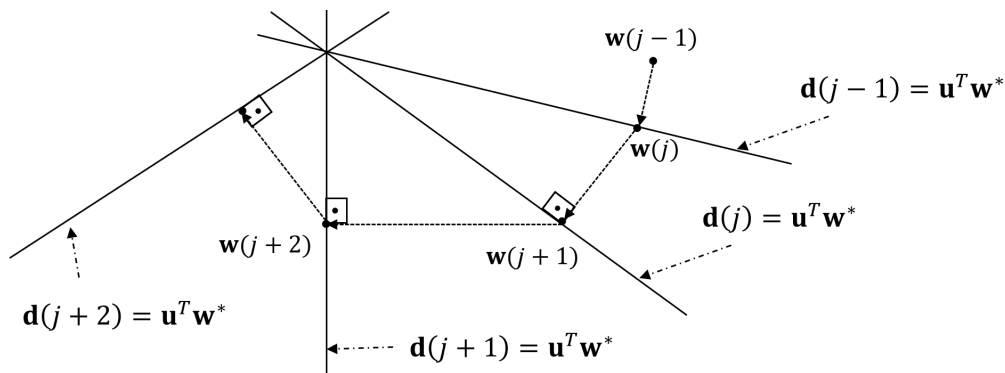


Figure 1: Geometric description of the NLMS projection in \mathbb{R}^2 .

provided that the intersection of the hyperplanes is non-empty Combettes (1993); Cetin et al. (2013).

Other distance measures lead to different update equations such as the ℓ_1 -norm-based updates:

$$\mathbf{w}(j) = \mathbf{w}(j-1) + \frac{\mathbf{e}(j)}{\|\mathbf{u}(j)\|_1} \mathbf{u}(j), \quad (9)$$

where $\|\mathbf{u}(j)\|_1$ is the ℓ_1 norm of the vector \mathbf{u}_j Gunay et al. (2012); Sayin et al. (2014); Arikan et al. (1994; 1995); Aydin et al. (1999). The ℓ_1 -norm-based method is usually more robust to outliers in input.

This article describes a new optimization algorithm inspired by Normalized LMS. It is called Input Normalized-SGD (INSGD) and utilizes the same approach as in NLMS. INSGD solves the constant learning rate issue that may cause divergence and obtains better accuracy results on benchmark datasets. The initialization of the learning rate or step size is crucial in DNN model training as it can greatly impact the convergence. We believe that incorporating the adaptive nature of NLMS into DNN training is a promising idea worth exploring. By adapting the concepts of NLMS to deep learning, we can potentially improve the convergence behavior and overall performance of DNN models.

2 Methodology

2.1 Motivation

Machine learning models commonly utilize the backpropagation method for optimization Rumelhart et al. (1986); LeCun et al. (1988). Stochastic Gradient Descent (SGD) is a widely used optimization algorithm with various modifications in the machine learning community. While SGD can provide convergence with proper initialization, researchers have identified both positive and negative aspects of SGD and have attempted to enhance it according to their specific objectives Ruder (2016). One issue with SGD is that it updates weights based solely on the instantaneous gradient, which may lead to a lack of global information and oscillations. Another challenge is the use of a constant learning rate for all weights in the model. As training progresses, certain weights become more important than others, requiring different step sizes to ensure effective learning.

In recent years, the Adaptive Gradient (AdaGrad) algorithm was introduced by Duchi *et al.* as a means to enhance the update term in optimization Duchi et al. (2011). AdaGrad addresses the issue of choosing an appropriate learning rate by adapting it individually for each weight based on the cumulative sum of past and current squared gradients. By dividing the learning rate by the square root of this cumulative sum, AdaGrad assigns larger updates to weights with smaller gradients and vice versa. This adaptive approach allows for a more fine-grained adjustment of the learning rate based on the historical behavior of each weight’s gradient. The formulas for AdaGrad are

$$\mathbf{w}(k+1) \leftarrow \mathbf{w}(k) - \frac{\gamma}{\sqrt{v(k) + \epsilon}} \nabla_{\mathbf{w}(k)} L, \quad (10)$$

$$v(k) \leftarrow v(k-1) + [\nabla_{\mathbf{w}(k)} L]^2, \quad (11)$$

where, v is the weighted moving average of the squared gradient, γ is the learning rate, and $v(-1) = 0$.

Hinton *et al.* introduced the RMSProp algorithm as an enhancement to the AdaGrad optimizer Hinton et al. (2012). RMSProp incorporates momentum by introducing an exponentially weighted moving average of the squared gradients. This modification helps to address the issue of diminishing learning rates in AdaGrad, which can slow down the convergence process. By applying the momentum concept, RMSProp allows for a smoother and more stable update process by considering not only the current squared gradients but also the historical information encapsulated in the moving average. As a result, RMSProp strikes a balance between the adaptability of AdaGrad and the stability provided by momentum, leading to improved optimization performance. RMSProp’s formulas are

$$\mathbf{w}(k+1) \leftarrow \mathbf{w}(k) - \frac{\gamma}{\sqrt{v(k) + \epsilon}} \nabla_{\mathbf{w}(k)} L, \quad (12)$$

$$v(k) \leftarrow \beta v(k-1) + (1 - \beta) [\nabla_{\mathbf{w}(k)} L]^2. \quad (13)$$

Another widely used optimization algorithm, called Adaptive Moment Estimation (Adam), was introduced by Kingma and Ba in 2014 Kingma & Ba (2014). Adam builds upon the concepts of momentum and the divisor factor used in RMSProp. In addition to maintaining an exponentially weighted moving average of the squared gradients like RMSProp, Adam also incorporates the notion of momentum by keeping track

of an exponentially weighted moving average of the gradients themselves. This combination of momentum and the divisor factor makes Adam more adaptive and robust compared to RMSProp and AdaGrad. By considering both the first and second moments of the gradients, Adam adjusts the learning rate for each parameter individually, taking into account both the magnitude and direction of the gradients. This enables Adam to converge faster and handle a wider range of optimization scenarios. The algorithm is implemented as:

$$\mathbf{w}(k+1) \leftarrow \mathbf{w}(k) - \frac{\gamma}{\sqrt{v(k)} + \epsilon} \mathbf{m}(k), \quad (14)$$

$$v(k) \leftarrow \beta v(k-1) + (1-\beta) [\nabla_{\mathbf{w}(k)} L]^2, \quad (15)$$

$$\mathbf{m}(k) \leftarrow \beta \mathbf{m}(k-1) + (1-\beta) \nabla_{\mathbf{w}(k)} L, \quad (16)$$

where \mathbf{m} is the momentum and $\mathbf{m}(-1) = \mathbf{0}$.

Another adaptive learning algorithm proposed by Singh *et al.* in Singh et al. (2015) presented a Layer-Specific Adaptive Learning Rate (LSALR). According to Singh et al. (2015), the parameters in the same layer share similar gradients; therefore, the learning rate of the entire layer should be similar but different layers should have different learning rates. The work is described to adjust the learning rate to escape from the saddle points and it uses the ℓ_2 norm in gradients:

$$\mathbf{w}(k+1) \leftarrow \mathbf{w}(k) - \gamma \left(1 + \log \left(1 + \frac{1}{\|\nabla_{\mathbf{w}(k)} L\|_2} \right) \right) \nabla_{\mathbf{w}(k)} L. \quad (17)$$

Eq. (17) allows the learning rate to become larger when the gradients are small. The aim is to correct the update term when the gradients are small in the high error low curvature saddle points. Therefore, the algorithm escapes from saddle points with a large learning rate. Similarly, it scales the learning rate to stability if the gradients are too large. The use of the *log* function provides the scaling under different conditions.

Adam, AdaGrad, and RMSProp are optimization algorithms that address the limitations of standard stochastic gradient descent (SGD). These algorithms aim to improve the convergence speed in various scenarios, such as high learning rates or random weight initializations. While they incorporate normalization parameters, the update terms in these algorithms are still input-dependent and gradually decrease over iterations. In our approach, we propose using a normalization term based on the layer’s input instead of relying on cumulative sums, which helps to prevent slow convergence. By leveraging input-based normalization, we aim to enhance the training process and overcome the limitations of existing optimization algorithms.

2.2 Input Normalized Stochastic Gradient Descent Algorithm

Input Normalized Stochastic Gradient Descent (INSGD) utilizes a similar approach as NLMS. The input scalability issue and the fragile nature of choosing the learning rate are the main issues that we address in the INSGD optimizer.

In deep learning, we minimize the cost function

$$F(\mathbf{W}) = \frac{1}{n} \sum_{k=1}^n F_k(\mathbf{W}),$$

where \mathbf{W} represents the parameters of the network, n is the number of training samples, and $F_k(\mathbf{W})$ is the loss due to the k -th training data. Let us first assume that there are linear neurons in the last layers of the network and d_i is the desired value of the i -th neuron. Furthermore, let $\mathbf{w}_{i,0}$ be the initial weights of the i -th neuron. We want the neuron to satisfy

$$d_i = \mathbf{w} \cdot \mathbf{x},$$

where \mathbf{x} denotes the input vector to the neuron. During training, we have $\mathbf{w}_{i,0} \cdot x_k \neq d_i$ where \mathbf{x}_k is the input vector due to the k -th training pattern. We select the new set of weights of the neuron by solving

$$\arg \min_{\mathbf{w}} \|\mathbf{w}_{i,0} - \mathbf{w}\|^2, \quad (18)$$

$$\text{s.t. } \mathbf{w} \cdot \mathbf{x}_k = d_i.$$

One can easily obtain the solution using the Lagrange multiplier method, and the solution to the optimization problem is the orthogonal projection onto the hyperplane $\mathbf{w} \cdot \mathbf{x}_k = d_i$. Solving Eq.(18) gives us an update equation

$$\mathbf{w}_{i,1} = \mathbf{w}_{i,0} + \lambda \frac{e_k}{\epsilon + \|\mathbf{x}_k\|^2} \mathbf{x}_k, \quad (19)$$

where the error $e_k = d_i - \mathbf{w}_{i,0} \cdot \mathbf{x}_k$, the update parameter $\lambda = 1$, and ϵ is a small number to avoid the division by 0. This selection of weights obviously reduces $F_k(\mathbf{W})$ and it is the same as the gradient descent with a new step size determined by the length of the input vector. It is also the well-known Normalized Least Mean Square (NLMS) algorithm used in adaptive filtering and signal processing as shown in Sec 1.2, Eq. (7). The NLMS algorithm converges for $0 < \lambda < 2$ when the input is a wide-sense stationary random process. Inspired by the NLMS algorithm we can continue updating the neurons of the inner layers of the network in the same manner.

When the i -th neuron is not a linear neuron, we have

$$\psi(\mathbf{w} \cdot \mathbf{x}) = d_i, \quad (20)$$

where $\psi(\cdot)$ is the activation function. In this case, we solve the following problem to update the weights of the neuron.

$$\begin{aligned} \arg \min_{\mathbf{w}} \|\mathbf{w}_{i,0} - \mathbf{w}\|^2, \\ \text{s.t. } \psi(\mathbf{w} \cdot \mathbf{x}_k) = d_i, \end{aligned} \quad (21)$$

or

$$\begin{aligned} \arg \min_{\mathbf{w}} \|\mathbf{w}_{i,0} - \mathbf{w}\|^2, \\ \text{s.t. } \mathbf{w} \cdot \mathbf{x}_k = \phi(d_i), \end{aligned} \quad (22)$$

where $\phi(\cdot)$ is the inverse of the $\psi(\cdot)$ function. When $\psi(\cdot)$ is the sigmoid, leaky-RELU, or tanh, $\psi(\cdot)$ has a well-defined inverse. If the activation function is ReLU, the negative values in the inverse are set to 0. In this case, the weight update equation will be

$$\mathbf{w}_{i,1} = \mathbf{w}_{i,0} + \lambda \frac{(\phi(d_i) - \mathbf{w}_{i,0} \cdot \mathbf{x}_k)}{\epsilon + \|\mathbf{x}_k\|^2} \mathbf{x}_k. \quad (23)$$

By employing the solution described in Eq. (23), the NLMS algorithm can be adapted to optimize the weights in the final layer to minimize various cost functions. However, extending the INSGD algorithm to deeper networks with multiple layers poses a challenge in its derivation. We adopt similar assumptions to those used in the backpropagation algorithm to derive the INSGD algorithm for each weight in a deep-learning model. These assumptions provide a foundation for developing the INSGD algorithm, allowing us to effectively optimize the weights across the layers of the deep learning model.

In addition to the final layer, we incorporate the input feature maps of each layer to apply the gradient term with normalization to the neurons using the backpropagation algorithm. This enables us to propagate the gradients and update the weights in a layer-wise manner throughout the network. By leveraging the information from the input feature maps, we enhance the training process by ensuring that the gradients are appropriately scaled and normalized at each layer. This approach allows for effective gradient propagation and weight updates, ultimately contributing to improved optimization and performance of the deep learning model:

$$\mathbf{w}_{k+1} = \mathbf{w}_k - \mu \frac{\nabla_{\mathbf{w}_k} L(\mathbf{e}_k)}{\epsilon + \|\mathbf{x}_k\|_2^2}, \quad (24)$$

where \mathbf{x}_k is the vector of inputs to the neuron and \mathbf{w}_k are the weights of the neurons. Note that we drop i in the weight notation that represents the neuron since the algorithm is applicable to every neuron. For convenience, we also change the notation for the learning rate from λ to μ . A description of how the INSGD optimizer algorithm works for any layer of a typical deep network is shown in Fig. 2.

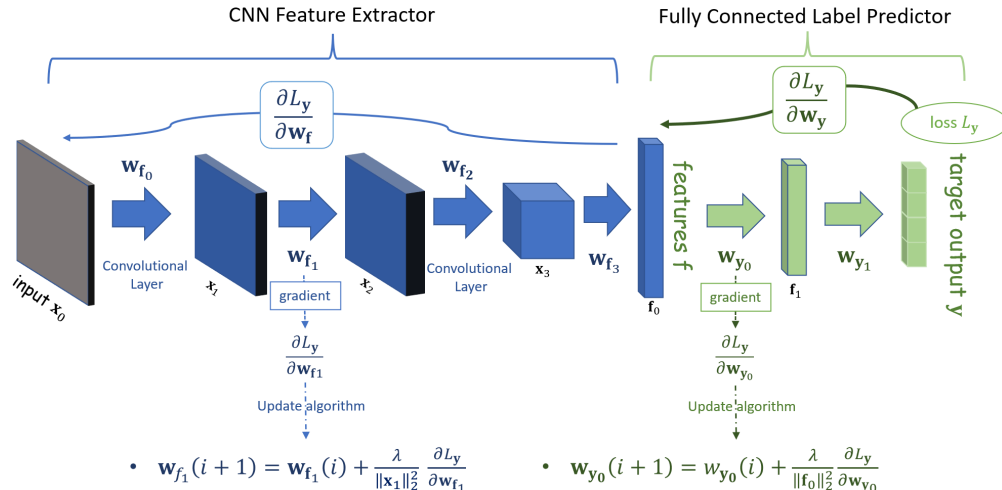


Figure 2: NSGD algorithm for different layers. It utilizes the input to each layer to update the weights.

The proposed INSGD algorithm, while addressing the input scalability problem, still shares some drawbacks with SGD. In Eq. (24), we can observe how the weights are updated based on the input and gradient at each time step. However, the presence of irregular gradients and outlier inputs from the training dataset can impact the convergence behavior. To overcome this, we incorporate momentum, a technique that aids in navigating high error and low curvature regions Ruder (2016). In the INSGD algorithm, we introduce an input momentum term to estimate the power of the dataset, enabling power normalization. By replacing the denominator term with the estimated input power, we emphasize the significance of power estimation in our algorithm. Furthermore, the utilization of input momentum allows us to capture the norm of all the inputs. Denoted as P , the input momentum term accumulates the squared ℓ_2 norm of the input instances:

$$P_k = \beta P_{k-1} + (1 - \beta) \|\mathbf{x}_k\|_2^2. \quad (25)$$

While estimating the input power is crucial, we encounter a challenge similar to AdaGrad. The normalization factor can grow excessively, resulting in infinitesimally small updates. To address this, we draw inspiration from the Layer Specific Adaptive Learning Rate (LSALR) approach Singh et al. (2015) and employ the logarithm function to stabilize the normalization factor. However, the use of the logarithm function introduces the risk of negative values. If the power is too low, the function could yield a negative value, reversing the direction of the update. To mitigate this, we employ a function with the rectified linear unit, which avoids the issue of negative values. Adding a regularizer may not be sufficient to resolve this problem, hence the choice of the rectified linear unit function. The function is designed as follows:

$$f_\epsilon(u) = \begin{cases} u & \text{if } u \geq \epsilon, \\ \epsilon & \text{if } u < \epsilon, \end{cases} \quad (26)$$

where ϵ is a regularizer to avoid the division by 0. After devising the function in Eq. (26) and the logarithm approach for the Eq. (25), the optimization algorithm for any weight in any layer in a network becomes

$$\mathbf{w}_{k+1} = \mathbf{w}_k - \frac{\mu}{f_\epsilon(\log(P_k))} \nabla_{\mathbf{w}_k} L(\mathbf{e}_k), \quad (27)$$

where P_k is defined in Eq. (25), and it is the estimate of the input power that is updated with every instance of \mathbf{x} and the proposed $\epsilon = 0.01$. Therefore, we make sure that the update term is always greater than 0 and stable. The iterative algorithm defined in Eq. (27) is the Input Normalized SGD algorithm.

One can explore different norms, such as the l_1 or l_∞ norm, as alternatives to the l_2 norm. In our experiments, we also investigated the use of the l_1 norm to assess its impact on performance. LMS algorithms based on the l_1 norm are known to be more robust against outliers in the input, which suggests potential benefits in

deep neural network training. In this study, we examined both the l_2 and l_1 norms and their implications. Since NLMS is based on the l_2 norm, the algorithm presented in Eq. (25) utilizes the l_2 norm. However, for broader applicability, we can adapt the power estimation as follows:

$$P_k = \beta P_{k-1} + (1 - \beta) \|\mathbf{x}_k\|_p^p \quad (28)$$

where $\|\cdot\|_p^p$ is the p power of the p -norm. Extension of the INSGD to convolutional layers is straightforward. The pseudocode algorithm of INSGD is given in Algorithm 1.

Algorithm 1 Input Normalized Gradient Descent with Momentum

```

for  $t \leftarrow 1$  to ... do
   $g_t \leftarrow \nabla_{\theta} f_t(\theta_{t-1})$  ▷ Denote the gradient
  if  $\beta \neq 0$  then ▷ If input momentum is not 0
    if  $t > 1$  then
       $P_t \leftarrow \beta P_{t-1} + (1 - \beta) \|\mathbf{x}_{t,\theta}\|_2^2$  ▷ Accumulate the power of input norm
    else
       $P_t \leftarrow \|\mathbf{x}_{t,\theta}\|_2^2$ 
    end if
  end if
   $g_t \leftarrow \frac{g_t}{f(\log(P_t))}$  ▷ Division by input norm
  if  $\lambda \neq 0$  then ▷ Weight Decay
     $g_t \leftarrow g_t + \lambda \theta_{t-1}$ 
  end if
  if  $\gamma \neq 0$  then ▷ Gradient with Momentum
    if  $t > 1$  then
       $\mathbf{b}_t \leftarrow \gamma \mathbf{b}_{t-1} + (1 - \gamma) g_t$ 
    else
       $\mathbf{b}_t \leftarrow g_t$ 
    end if
     $g_t \leftarrow \mathbf{b}_t$ 
  end if
   $\theta_t \leftarrow \theta_{t-1} - \mu g_t$  ▷ Update the Weights
end for

```

2.3 Models Architecture

In this study, we conducted experiments using five different networks to evaluate the performance of the INSGD algorithm in the classification tasks of CIFAR-10, CIFAR-100, and ImageNet-1K. We made modifications to the network architectures and initialization settings to assess the impact of the INSGD algorithm. In this study, we employed several networks for the classification tasks. Specifically, we utilized ResNet-20 He et al. (2016) and MobileNetV3 Howard et al. (2019) for CIFAR-10, WResNet-18 Zagoruyko & Komodakis (2016) for CIFAR-100, ResNet-50 and MobileNetV3 for ImageNet-1K. Additionally, we designed a custom CNN architecture specifically for CIFAR-10, which consists of four convolutional layers, each followed by a batch normalization layer. These networks were chosen to provide a diverse set of architectures and enable a comprehensive evaluation of the INSGD algorithm’s performance across different datasets. The structure of ResNet-20 and custom-designed CNN used in this study is shown in Tables 1 and 2.

On large benchmark datasets, traditional optimization algorithms often struggle to find the optimum results if the learning rate is not properly chosen. In such cases, these algorithms may diverge and fail to converge to the desired solution. However, the INSGD algorithm offers a solution by providing flexibility in learning

Layer	Output Shape	Implementation Details
Conv1	$16 \times 32 \times 32$	$3 \times 3, 16$
Conv2_x	$16 \times 32 \times 32$	$\left[\begin{array}{c} 3 \times 3, 16 \\ 3 \times 3, 16 \end{array} \right] \times 3$
Conv3_x	$32 \times 16 \times 16$	$\left[\begin{array}{c} 3 \times 3, 32 \\ 3 \times 3, 32 \end{array} \right] \times 3$
Conv4_x	$64 \times 8 \times 8$	$\left[\begin{array}{c} 3 \times 3, 32 \\ 3 \times 3, 64 \end{array} \right] \times 3$
GAP	64	Global Average Pooling
Output	10	Linear

Table 1: ResNet-20 Structure for CIFAR-10 classification task. Building blocks are shown in brackets, with the numbers of blocks stacked. Downsampling is performed by Conv3_1 and Conv4_1 with a stride of 2.

Layer	Output Shape	Implementation Details
Conv1	$8 \times 32 \times 32$	$3 \times 3, 8$
Conv2	$16 \times 16 \times 16$	$3 \times 3, 16, \text{stride} = 2$
Conv3	$32 \times 8 \times 8$	$3 \times 3, 32, \text{stride} = 2$
Conv4	$64 \times 4 \times 4$	$3 \times 3, 64, \text{stride} = 2$
Dropout	$64 \times 4 \times 4$	$p = 0.2$
Flatten	1024	-
Output	10	Linear

Table 2: Structure of the custom network with 4 conv layers for the CIFAR-10 classification task.

rate selection, thereby improving the chances of reaching the global optimum. By adapting the learning rate dynamically based on the input and gradient information, INSGD enhances the optimization process and increases the likelihood of achieving superior results on large-scale datasets.

3 Experimental Results

Our experiments are carried out on a workstation with an NVIDIA GeForce GTX 1660 Ti GPU for the CIFAR-10 and a workstation with an NVIDIA RTX A6000 GPU for the CIFAR-100 and ImageNet-1K.

3.1 CIFAR-10 Classification

We conduct a series of experiments using the CIFAR-10 dataset which consists of 10 classes, initially employing the custom-designed CNN and ResNet-20 models for training. In certain experiments, we make modifications to the custom network to explore the algorithm’s capabilities. These experiments aim to assess the algorithm’s performance under various conditions.

The base setting employed the SGD optimizer with a weight decay of 0.0005 and a momentum of 0.9. The models are trained using a mini-batch size of 128 for 200 epochs, with an initial learning rate ranging from 0.5 to 0.01. The learning rate is reduced at multiple steps with varying rates. To augment the data, we perform padding of 4 pixels on the training images, followed by random crops to obtain 32x32 images. Random horizontal flips are also applied to the images with a probability of 0.5. Normalization is performed on the images using a mean of [0.4914, 0.4822, 0.4465] and a standard deviation of [0.2023, 0.1994, 0.2010]. Throughout the training process, the best models are saved based on their accuracy on the CIFAR-10 test dataset. These settings are adopted from He et al. (2016).

In the initial experiment, we employ the ResNet-20 model as our baseline. The independent parameter in this experiment is the learning rate, which is varied across different settings. The batch size is fixed at 128. We compare the accuracy results of our algorithm against those of other commonly used optimization algorithms, which are discussed in Section 2.1. The detailed accuracy results are presented in Table 3.

Optimizer	Initial Learning Rate	Test Accuracy
SGD	0.01	90.95%
SGD	0.1	92.55%
Adam	0.001	91.39%
Adagrad	0.01	87.29%
Adagrad	0.1	89.41%
Adadelata	0.1	89.33%
INSGD- ℓ_1	0.01	90.80%
INSGD- ℓ_1	0.1	92.64%
INSGD- ℓ_2	0.01	91.28%
INSGD- ℓ_2	0.1	92.77%

Table 3: Accuracy results of ResNet-20 on the CIFAR-10 dataset with different initial learning rates using different optimization algorithms.

In addition to showcasing the testing accuracy results, understanding the behavior of each optimizer throughout the training process is crucial. Figure 3 visually represents the progression of testing set errors for each optimizer over 200 epochs. By training the ResNet-20 model with each optimizer, we can observe the corresponding testing set error depicted in the plot. This visualization offers valuable insights into the convergence speed and overall behavior of each optimizer, enabling a comprehensive analysis of their performance and effectiveness.

As depicted in Figure 3, the INSGD algorithm with both norms consistently exhibits lower error rates in the testing set, outperforming the other optimizers. This indicates the superior performance and effectiveness of INSGD in optimizing the model’s parameters and minimizing the testing set errors. The ability of INSGD to adaptively adjust the learning rates for each individual parameter contributes to its remarkable performance in achieving lower errors during the training process. Such results further validate the efficacy of the INSGD algorithm and its potential as an efficient optimizer for deep learning tasks.

Table 3 clearly illustrates the significant improvement in accuracy achieved by the INSGD algorithm compared to other traditional optimization algorithms, resulting in better convergence during the CIFAR-10 training. It is important to note that INSGD consistently performs at a high level across various initial learning rates. The superior performance of INSGD highlights its potential as a robust optimization algorithm for deep learning tasks, showcasing its effectiveness in addressing the challenge of tuning learning rates and achieving improved convergence.

In the second experiment, we explore the impact of varying batch sizes on the normalization factor to understand how input size affects the training process. Analyzing the results across different batch sizes is crucial due to the trade-off between time and memory usage. While larger datasets may benefit from larger batch sizes to expedite training time, it is important to consider the increased memory requirements. If our algorithm produces comparable results with larger batch sizes, it demonstrates its scalability. Table 4 presents the accuracy results of other algorithms and INSGD when training the model with different batch sizes. To accommodate the increased batch size, we adjust the learning rate according to the linear scaling rule described in Goyal et al. (2017).

To enhance the diversity of models utilized in our experiments, we incorporate the MobileNetV3 model for comparative analysis. A batch size of 256 is used in MobileNetV3 training. As depicted in Table 5, the results

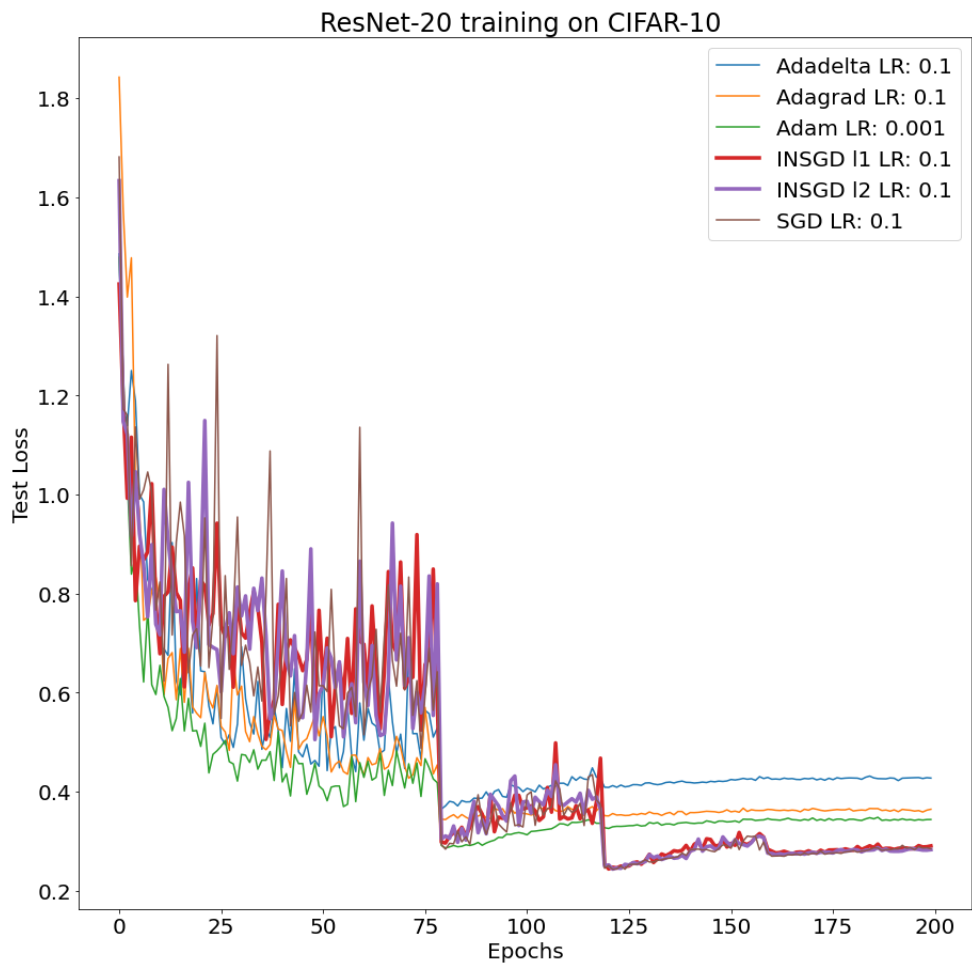


Figure 3: Testing set error of each optimizer over 200 epochs

Optimizer	Batch	Learning Rate	Test Accuracy
SGD	128	0.1	92.55%
INSGD- l_1	128	0.1	92.64%
INSGD- l_2	128	0.1	92.77%
SGD	256	0.2	92.46%
INSGD- l_1	256	0.2	92.19%
INSGD- l_2	256	0.2	92.56%
SGD	512	0.2	92.20%
INSGD- l_1	512	0.2	92.39%
INSGD- l_2	512	0.2	92.80%

Table 4: Accuracy results of the ResNet-20 on the CIFAR-10 dataset with different batch sizes.

clearly demonstrate that the INSGD algorithm outperforms other conventional optimization algorithms in terms of performance. This finding highlights the superior capabilities of INSGD in achieving improved outcomes across the evaluated metrics.

Optimizer	Initial Learning Rate	Test Accuracy
Adam	0.001	89.93%
Adagrad	0.1	87.23%
Adadelta	0.1	86.32%
SGD	0.1	90.83%
INSGD- ℓ_1	0.1	90.94%
INSGD- ℓ_2	0.1	91.13%

Table 5: Accuracy results of MobileNetV3 on the CIFAR-10 dataset with different initial learning rates using different optimization algorithms.

We also conduct experiments using the custom network for the CIFAR-10 training to validate our algorithm. We employed similar settings to those used in ResNet-20. The accuracy results of the custom network with different initial learning rates are presented in Table 6.

Optimizer	Initial Learning Rate	Test Accuracy
SGD	0.1	78.63%
INSGD- ℓ_1	0.1	79.35%
INSGD- ℓ_2	0.1	78.76%
SGD	0.25	64.34%
INSGD- ℓ_1	0.25	70.64%
INSGD- ℓ_2	0.25	73.06%
SGD	0.05	79.19%
INSGD- ℓ_1	0.05	79.11%
INSGD- ℓ_2	0.05	79.62%
SGD	0.01	77.51%
INSGD- ℓ_1	0.01	78.79%
INSGD- ℓ_2	0.01	79.26%

Table 6: Accuracy results of the custom-designed CNN on the CIFAR-10 dataset with different initial learning rates and reduction rates.

The toy network, used as a simplified representation of the model, plays a crucial role in evaluating the effectiveness of our algorithm. The results obtained from training the toy network confirm the robustness of INSGD, as it consistently improves the accuracy regardless of the network architecture or the learning rate used. This highlights the flexibility of INSGD as an optimizer, allowing for the utilization of various learning rates. Notably, when compared to SGD with momentum, INSGD consistently achieves superior performance across various learning rates, underscoring its efficacy in optimizing model training. Given the overlap in the experiments conducted with the custom network and ResNet-20, we opted not to replicate the ResNet-20 experiments using the toy network. This decision was made to avoid redundancy in our findings and to focus on exploring the direct impact of INSGD

3.2 CIFAR-100 Experiment

We further extend our research by conducting experiments on the CIFAR-100 dataset. CIFAR-100 is a more challenging dataset compared to CIFAR-10 as it contains 100 classes instead of 10, requiring models

to have a higher level of discrimination and classification capability. The increased class diversity in CIFAR-100 poses additional difficulty in achieving high accuracy and generalization performance. It is crucial to ensure that each class is adequately represented in the training process. Hence, we also opted to increase the batch size to 256 for this particular experiment. Before our study, Wide ResNet-18 was recognized for its convergence capabilities and satisfactory results Zagoruyko & Komodakis (2016). In alignment with the settings outlined in the Wide ResNet paper, we replaced the optimizer algorithm with INSGD. Similar to our CIFAR-10 experiment, the model was trained for 200 epochs, and we report the highest accuracy achieved on the testing data.

Optimizer	LR	Batch	Top-1 Acc.	Top-5 Acc.
SGD	0.1	128	78.75%	94.20%
INSGD- ℓ_1	0.1	128	78.52%	94.66%
INSGD- ℓ_2	0.1	128	78.85%	94.34%
SGD	0.1	256	77.22%	93.79%
INSGD- ℓ_1	0.1	256	78.15%	94.54%
INSGD- ℓ_2	0.1	256	77.89%	93.98%

Table 7: Accuracy results of the Wide ResNet-18 on the CIFAR-100 dataset.

The results presented in Table 7 provide compelling evidence of the effectiveness of the INSGD algorithm in achieving improved convergence on complex datasets across a range of learning rates. The superior performance of INSGD, as evidenced by its higher Top-1 and Top-5 accuracy, establishes its utility in training sophisticated models on challenging datasets. These findings underscore the algorithm’s capability to handle intricate data distributions and optimize model performance, thereby showcasing its potential for advancing the state-of-the-art in deep learning.

3.3 ImageNet-1K Results

In this subsection, we present the test accuracy results on the ImageNet-1K dataset. We utilize the ResNet-50 model, as discussed in Section 2.3. The training process is conducted using the official PyTorch ImageNet-1K training code Ima (2022). Specifically, we employ the SGD and INSGD optimizers with a weight decay of 0.0001 and a momentum of 0.9.

The ImageNet-1K dataset consists of 1.2 million images and is known for its difficulty in training. Due to the image resolution and resource constraints, adopting larger batch sizes is not feasible in our environment. As a result, we train the models with a mini-batch size of 256, an initial learning rate of 0.1 for 90 epochs, and a learning rate reduction of 1/10 after every 30 epochs.

To augment the data, we perform random cropping and horizontal flipping with a probability of 0.5, resulting in 224×224 images. The images are then normalized using a mean of [0.485, 0.456, 0.406] and a standard deviation of [0.229, 0.224, 0.225].

The accuracy of the best models is presented in Table 8, based on the center-crop top-1 accuracy and top-5 accuracy on the ImageNet-1K validation dataset. These accuracies are obtained from the model with the highest center-crop top-1 accuracy, providing a comprehensive evaluation of the model’s performance on the ImageNet-1K dataset.

The results presented in Table 8 highlight the improved top-1 accuracy achieved by the INSGD algorithm on the ImageNet-1K dataset. This improvement is particularly significant considering the scale of the dataset, demonstrating the effectiveness of INSGD in handling large and complex datasets. By leveraging the input normalization factor, INSGD enables the model to converge more effectively by aligning the gradient direction and appropriate magnitude.

The power estimation obtained through momentum in INSGD indicates that the optimization algorithm can benefit from considering the entire input sequence. It suggests that the algorithm can capture long-

Optimizer	Learning Rate	Top-1 Acc.	Top-5 Acc.
Model: ResNet-50			
SGD	0.05	75.20%	92.49%
SGD	0.1	75.56%	92.53%
INSGD- ℓ_1	0.05	75.59%	92.74%
INSGD- ℓ_1	0.1	75.77%	92.71%
INSGD- ℓ_2	0.05	75.67%	92.66%
INSGD- ℓ_2	0.1	75.89%	92.81%
Model: MobileNet V3			
SGD	0.05	66.94%	87.48%
INSGD- ℓ_2	0.05	68.15%	88.12%

Table 8: Accuracy results of ResNet-50 and MobileNetV3 on the ImageNet-1K dataset.

term dependencies and utilize them for better optimization performance. Furthermore, it is worth noting that the batch size used in our experiments is relatively small compared to the number of images in the dataset. Exploring the algorithm’s behavior with larger batch sizes would be an interesting avenue for future investigation.

4 Conclusion

In this paper, we proposed a novel neural network training method called INSGD, which incorporates ideas from the widely used NLMS algorithm in adaptive filtering. INSGD introduces a normalization step to the weight update term that normalizes the update term using only the input vector to the neurons. The normalization can be performed using both the l_1 and l_2 norms.

To evaluate the effectiveness of INSGD, we conducted experiments on various datasets using different models. Notably, our algorithm consistently demonstrated improvements in testing accuracy across multiple datasets. For example, on the CIFAR-10 dataset, INSGD achieved a significant boost in accuracy compared to traditional stochastic gradient algorithms. We observed similar positive outcomes on other datasets, such as CIFAR-100 and ImageNet-1K, when employing different models like ResNet-20 and ResNet-50.

Traditional optimization algorithms often lack flexibility when it comes to selecting hyperparameters, which can limit their effectiveness. However, the INSGD (Input Normalized Stochastic Gradient Descent) algorithm overcomes this limitation by leveraging input normalization. By normalizing the input data, INSGD enables greater flexibility in tuning hyperparameters, leading to more robust and stable performance.

The promising results obtained across diverse datasets and models validate the effectiveness of INSGD in enhancing the training process. By incorporating the normalization factor into the stochastic gradient algorithm, INSGD effectively leverages the benefits of the NLMS algorithm, leading to improved performance in various object recognition scenarios.

References

Steepest-Descent Technique, chapter 8, pp. 138–147. John Wiley & Sons, Ltd, 2008. ISBN 9780470374122. doi: <https://doi.org/10.1002/9780470374122.ch15>. URL <https://onlinelibrary.wiley.com/doi/abs/10.1002/9780470374122.ch15>.

Imagenet training in pytorch. <https://github.com/pytorch/examples/tree/main/imagenet>, 2022. Accessed: 2022-12-27.

- O. Arikan, A. Enis Cetin, and E. Erzin. Adaptive filtering for non-gaussian stable processes. *IEEE Signal Processing Letters*, 1(11):163–165, 1994. doi: 10.1109/97.335063.
- O. Arikan, M. Belge, A.E. Cetin, and E. Erzin. Adaptive filtering approaches for non-gaussian stable processes. In *1995 International Conference on Acoustics, Speech, and Signal Processing*, volume 2, pp. 1400–1403 vol.2, 1995. doi: 10.1109/ICASSP.1995.480503.
- G. Aydin, O. Arikan, and A.E. Cetin. Robust adaptive filtering algorithms for α -stable random processes. *IEEE Transactions on Circuits and Systems II: Analog and Digital Signal Processing*, 46(2): 198–202, 1999. doi: 10.1109/82.752953.
- Léon Bottou. Large-scale machine learning with stochastic gradient descent. In *Proceedings of COMP-STAT'2010: 19th International Conference on Computational Statistics Paris France, August 22-27, 2010 Keynote, Invited and Contributed Papers*, pp. 177–186. Springer, 2010.
- A Enis Cetin, Omer N Gerek, and Yasemin Yardimci. Equiripple fir filter design by the fft algorithm. *IEEE Signal Processing Magazine*, 14(2):60–64, 1997.
- A Enis Cetin, Alican Bozkurt, Osman Gunay, Yusuf Hakan Habiboglu, Kivanc Kose, Ibrahim Onaran, Mohammad Tofghi, and Rasim Akin Sevimli. Projections onto convex sets (pocs) based optimization by lifting. In *2013 IEEE Global Conference on Signal and Information Processing*, pp. 623–623. IEEE, 2013.
- SC Chan and Yi Zhou. Convergence behavior of nlms algorithm for gaussian inputs: Solutions using generalized abelian integral functions and step size selection. *Journal of Signal Processing Systems*, 59(3): 255–265, 2010.
- Patrick L Combettes. The foundations of set theoretic estimation. *Proceedings of the IEEE*, 81(2):182–208, 1993.
- John Duchi, Elad Hazan, and Yoram Singer. Adaptive subgradient methods for online learning and stochastic optimization. *Journal of machine learning research*, 12(7), 2011.
- Priya Goyal, Piotr Dollár, Ross Girshick, Pieter Noordhuis, Lukasz Wesolowski, Aapo Kyrola, Andrew Tulloch, Yangqing Jia, and Kaiming He. Accurate, large minibatch sgd: Training imagenet in 1 hour. *arXiv preprint arXiv:1706.02677*, 2017.
- Osman Gunay, Behçet Ugur Toreyin, Kivanc Kose, and A. Enis Cetin. Entropy-functional-based online adaptive decision fusion framework with application to wildfire detection in video. *IEEE Transactions on Image Processing*, 21(5):2853–2865, 2012. doi: 10.1109/TIP.2012.2183141.
- Kaiming He, Xiangyu Zhang, Shaoqing Ren, and Jian Sun. Deep residual learning for image recognition. In *Proceedings of the IEEE conference on computer vision and pattern recognition*, pp. 770–778, 2016.
- Geoffrey Hinton, Nitish Srivastava, and Kevin Swersky. Neural networks for machine learning lecture 6a overview of mini-batch gradient descent. *Cited on*, 14(8):2, 2012.
- Geoffrey E Hinton and Ruslan R Salakhutdinov. Reducing the dimensionality of data with neural networks. *science*, 313(5786):504–507, 2006.
- Andrew Howard, Mark Sandler, Grace Chu, Liang-Chieh Chen, Bo Chen, Mingxing Tan, Weijun Wang, Yukun Zhu, Ruoming Pang, Vijay Vasudevan, et al. Searching for mobilenetv3. In *Proceedings of the IEEE/CVF international conference on computer vision*, pp. 1314–1324, 2019.
- Diederik P Kingma and Jimmy Ba. Adam: A method for stochastic optimization. *arXiv preprint arXiv:1412.6980*, 2014.
- Alex Krizhevsky, Ilya Sutskever, and Geoffrey E Hinton. Imagenet classification with deep convolutional neural networks. *Communications of the ACM*, 60(6):84–90, 2017.

- Quoc V Le, Jiquan Ngiam, Adam Coates, Abhik Lahiri, Bobby Prochnow, and Andrew Y Ng. On optimization methods for deep learning. In *Proceedings of the 28th International Conference on International Conference on Machine Learning*, pp. 265–272, 2011.
- Yann LeCun, D Touresky, G Hinton, and T Sejnowski. A theoretical framework for back-propagation. In *Proceedings of the 1988 connectionist models summer school*, volume 1, pp. 21–28, 1988.
- Yann LeCun, Yoshua Bengio, et al. Convolutional networks for images, speech, and time series. *The handbook of brain theory and neural networks*, 3361(10):1995, 1995.
- Xiaoyu Li and Francesco Orabona. On the convergence of stochastic gradient descent with adaptive stepsizes. In *The 22nd international conference on artificial intelligence and statistics*, pp. 983–992. PMLR, 2019.
- Jonathan Long, Evan Shelhamer, and Trevor Darrell. Fully convolutional networks for semantic segmentation. In *Proceedings of the IEEE conference on computer vision and pattern recognition*, pp. 3431–3440, 2015.
- V John Mathews and Zhenhua Xie. A stochastic gradient adaptive filter with gradient adaptive step size. *IEEE transactions on Signal Processing*, 41(6):2075–2087, 1993.
- Sebastian Ruder. An overview of gradient descent optimization algorithms. *arXiv preprint arXiv:1609.04747*, 2016.
- David E Rumelhart, Geoffrey E Hinton, and Ronald J Williams. Learning representations by back-propagating errors. *nature*, 323(6088):533–536, 1986.
- Ali H. Sayed. *Normalized LMS Algorithm*, chapter 11, pp. 178–182. John Wiley & Sons, Ltd, 2008. ISBN 9780470374122. doi: <https://doi.org/10.1002/9780470374122.ch18>. URL <https://onlinelibrary.wiley.com/doi/abs/10.1002/9780470374122.ch18>.
- Muhammed O. Sayin, N. Denizcan Vanli, and Suleyman Serdar Kozat. A novel family of adaptive filtering algorithms based on the logarithmic cost. *IEEE Transactions on Signal Processing*, 62(17):4411–4424, 2014. doi: 10.1109/TSP.2014.2333559.
- Karen Simonyan and Andrew Zisserman. Very deep convolutional networks for large-scale image recognition. *arXiv preprint arXiv:1409.1556*, 2014.
- Bharat Singh, Soham De, Yangmuzi Zhang, Thomas Goldstein, and Gavin Taylor. Layer-specific adaptive learning rates for deep networks. In *2015 IEEE 14th International Conference on Machine Learning and Applications (ICMLA)*, pp. 364–368. IEEE, 2015.
- Sergios Theodoridis, Konstantinos Slavakis, and Isao Yamada. Adaptive learning in a world of projections. *IEEE Signal Processing Magazine*, 28(1):97–123, 2010.
- H Trussell and M Civanlar. The feasible solution in signal restoration. *IEEE Transactions on Acoustics, Speech, and Signal Processing*, 32(2):201–212, 1984.
- Bernard Widrow, Marcian E Hoff, et al. Adaptive switching circuits. In *IRE WESCON convention record*, volume 4, pp. 96–104. New York, 1960.
- Isao Yamada, Konstantinos Slavakis, and Kenyu Yamada. An efficient robust adaptive filtering algorithm based on parallel subgradient projection techniques. *IEEE Transactions on Signal Processing*, 50(5): 1091–1101, 2002.
- Sergey Zagoruyko and Nikos Komodakis. Wide residual networks. *arXiv preprint arXiv:1605.07146*, 2016.